

Cobalt hexacyanoferrate modified microband gold electrode and its electrocatalytic activity for oxidation of NADH

Chen-Xin Cai^{*}, Huang-Xian Ju, Hong-Yuan Chen

Department of Chemistry, Nanjing University, Nanjing 210093, China

Received 11 April 1995; in revised form 22 May 1995

Abstract

A stable electroactive thin film of cobalt hexacyanoferrate (CoHCF) was electrochemically deposited on the surface of a microband gold electrode. The cyclic voltammograms of CoHCF film indicate the presence of two redox peaks corresponding to the hexacyanoferrate(II/III) redox couple. The electrochemical behaviour of CoHCF is related to the concentration of supporting electrolyte and counter-ions. The modified electrode shows excellent electrocatalytic activity towards the oxidation of reduced nicotinamide adenine dinucleotide (NADH) in phosphate buffer solution (pH 7.0), with an overpotential ca. 310–370 mV lower than that of the bare microband gold electrode. The catalytic peak current is proportional to NADH concentration in the range 0.5–6.0 mM with a correlation coefficient of 0.98. The catalytic rate constant of the modified electrode for the oxidation of NADH is determined using a rotating-disc electrode. The mechanism of the oxidation of NADH catalysed by the electrode is discussed.

Keywords: Microelectrodes; Catalytic methods; Electrocatalytic oxidation; NADH; Cobalt hexacyanoferrate

1. Introduction

Recently, various inorganic materials such as clays [1], zeolite [2], transition metal oxides [3], transition metal particles [4], polyoxometallates [5] and polynuclear transition metal hexacyanometallates [6–8] have been used to fabricate chemically modified electrodes which have potential applications such as electrode coating material for electrochromic displays [9], ion selective electrodes [10] and solid-state batteries [11]. Of these, the transition metal hexacyanoferrates, namely Prussian blue (PB) and its analogues, are an important class of insoluble mixed-valence polynuclear compounds because they can produce well-characterized electroactive films with properties in common not only with redox and ion-exchange polymers but also with intercalation compounds. Much research work has been published on PB-modified electrodes, but these have been few studies of electrodes modified by PB analogues. In this paper, we report the formation of cobalt hexacyanoferrate (CoHCF) thin film on the surface of a microband gold electrode and the electrocatalytic activity

of the CoHCF-modified microband gold electrode (CoHCF|Au) towards the oxidation of NADH.

The electrochemical oxidation of NADH is of increasing interest in developing amperometric enzyme electrodes for substrates which are enzymatically coupled to NAD^+/NADH [12] or in the electrochemical regeneration of the cofactor for enzymatically coupled biotransformations [13]. The amperometric electrodes combine the specificity and selectivity of biological molecules with the direct transduction of reaction rate into current response and represent powerful tools in the field of analysis and biotechnology. However, the oxidation of NADH at the bare electrode surface is highly irreversible. The reaction takes place at considerable overpotential and involves radical intermediates which cause electrode fouling [14]. To overcome these problems, modification of the electrode with redox mediators has been investigated extensively as a means of reducing the overpotential of the oxidation of NADH. Johansson, Gorton and coworkers have reported the electrocatalytic oxidation of NADH by adsorbed aromatics containing catechol functionalities [15,16] and adsorbed phenoxazines [17–20]. Albery and Bartlett [21] reported the oxidation of NADH on electrodes made of a conducting organic salt. Other mediators, such as 1,2-quinones [22–24], 1,4-quinones [25], alkylphenazinium

^{*} Corresponding author. Present address: Department of Chemistry, Nanjing Normal University, Nanjing 210097, China.

ions [26] and thionine [27], have been immobilized on the surface of carbon electrodes through covalent binding and direct adsorption, or chemically cross-linked using a polymer, and used to catalyse the oxidation of NADH. The electrocatalytic oxidation of NADH at electrodes modified with conducting polymers, such as poly(3-methylthiophene) [28], poly(mercaptoquinone) [29], poly(thionine) [30] and poly(metallophthalocyanine) [31], have also been reported recently.

Microelectrodes have received considerable attention in some applications owing to their many advantages compared with conventionally sized electrodes and have attracted great interest for the determination of biomolecules in small volumes. Although there have been many studies of the electrochemical oxidation of NADH using various electrodes [15–31], to our knowledge there are no reports of the electrochemical oxidation of NADH at a gold microelectrode. In order to obtain more redox information about NADH, the mechanism of the electrocatalytic oxidation of NADH at chemically modified electrodes and the development of a microsensor which depends on NADH for in-vivo analysis and biotechnology were investigated. It is also necessary to study the electrochemical oxidation of NADH at microelectrodes. The aim of this paper is to describe the voltammetric behaviour of NADH at a CoHCF|Au electrode and the electrochemical performance of the electrode. The inorganic films are stable in the electrochemical processes. A noticeable decrease in the overpotential for NADH oxidation and a remarkably stable voltammetric response at the modified electrode was observed. CoHCF appears to be ideal for applications in amperometric sensors.

2. Experimental

2.1. Chemicals

NADH was obtained from the Sigma Chemical Company and used as received. All other chemicals were of analytical grade. All solutions were prepared with doubly deionized water. The buffer solution (0.1 M) was made up from Na_2HPO_4 and NaH_2PO_4 (abbreviated as 0.1 M NaPB solution hereafter), K_2HPO_4 and KH_2PO_4 (abbreviated as 0.1 M KPB solution hereafter) or NaOAc and HOAc.

2.2. Apparatus

A three-electrode system with a platinum wire counter-electrode, a saturated calomel reference electrode (SCE) and a microband gold working electrode (ca. $0.1 \mu\text{m} \times 1.0 \text{cm}$) was employed. The method of fabrication of the microband gold electrode was the same as reported previously [32]. The working electrode was polished with 0.05 μm alumina slurry, rinsed with water and then cleaned in

ultrasonic cleaner with acetone and water. Prior to use, the electrode was pretreated by continuous cycling from 0 V to -2.0V at 50mV s^{-1} in phosphate buffer solution (pH 7.0) until a constant background was observed.

Electrochemical experiments were performed with a PAR M270 electrochemistry system (EG & G). Rotating-disc electrode measurements were carried out with a PAR M636 ring-disc electrode system (EG & G) using a gold disc electrode ($\Phi = 4.5 \text{mm}$). The gold disc electrode was treated in the same way as the microband gold electrode.

2.3. Procedures

The cobalt hexacyanoferrate film was electrochemically deposited on the microband gold electrode in the following manner, which is similar to that described in the literature [33]. The gold electrode was scanned from -0.5 to -1.15V at a rate of 10mV s^{-1} in 0.1 M KCl solution containing $1 \times 10^{-4} \text{M}$ CoCl_2 , and kept at a potential of -1.15V for a certain period of time for the deposition of cobalt. After removal from the solution and thorough rinsing with water, the electrode was dipped into a 0.2 M NaOAc + HOAc buffer solution (pH 4.7) containing $2 \times 10^{-3} \text{M}$ $\text{K}_3\text{Fe}(\text{CN})_6$, and scanned from -0.8 to $+0.4 \text{V}$ at 10mV s^{-1} . Finally, the electrode was rinsed thoroughly with water, and dipped into the phosphate buffer solution to study its electrochemical behaviour and examine the electrocatalytic activity for oxidation of NADH.

All the experiments were carried out at $25 \pm 0.1^\circ\text{C}$ under a N_2 atmosphere after deaerating with pure N_2 for 30 min. All the electrochemical experiments were performed inside a Faraday cage.

3. Results and discussion

3.1. Electrochemical behaviour of the CoHCF|Au electrode

Fig. 1(A) shows the voltammograms of a CoHCF|Au microelectrode in 0.1 M NaPB solution (pH 7.0) at various scan rates. Two well-defined redox peaks can be seen. Because the cobalt cannot be reduced in this potential range, the redox peaks correspond to the redox couple of hexacyanoferrate(II/III). The formal potential of $+0.33 \text{V/SCE}$ is obtained by averaging the cathodic and anodic peak potentials. The ratio of anodic to cathodic peak currents obtained at various scan rates is almost unity. The anodic and cathodic currents increase linearly with scan rate up to 200mV s^{-1} as shown in the inset to Fig. 1(A). The cyclic voltammogram is fully symmetric at $+0.33 \text{V}$ and no separation of peaks is observed at low scan rate ($< 20 \text{mV s}^{-1}$). A further increase in scan rate results in a separation of peaks; for example, a separation of ca. 21 mV occurs at 200mV s^{-1} . The apparent rate constant of CoHCF at the Au electrode surface, which was obtained

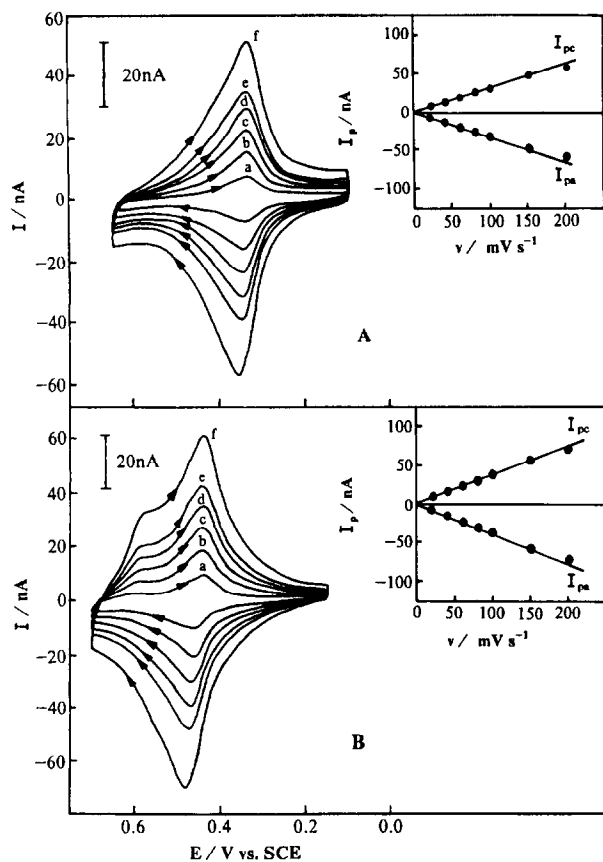


Fig. 1. Cyclic voltammograms of a CoHCF|Au microband electrode in (A) 0.1 M NaPB and (B) 0.1 M KPB solutions (pH 7.0) at a scan rate of (a) 20, (b) 40, (c) 60, (d) 80, (e) 100 and (f) 150 mV s^{-1} . The inset shows the dependence of peak currents on the scan rate.

using Laviron's method [34], is 3.1 s^{-1} . The half peak width is about $93 \pm 3 \text{ mV}$, which almost coincides with the theoretical value of a one-electron reaction mechanism process [35]. The surface coverage Γ can be evaluated from the equation

$$\Gamma = Q/nFA \quad (1)$$

where Q is the charge obtained by integrating the anodic peak under the background correction and the other symbols have their usual meanings. In the present case, Γ is $5.0 \times 10^{-8} \text{ mol cm}^{-2}$.

3.2. Effect of ions on the CoHCF|Au electrode

The electrochemical behaviour of CoHCF is mainly affected by cations, and anions have little effect. Fig. 1(B) shows the cyclic voltammograms of CoHCF|Au in 0.1 M KPB solution at various scan rates. The formal potential of CoHCF in 0.1 M KPB solution is $+0.45 \text{ V/SCE}$, which shifts in the positive direction by about 120 mV compared with that in 0.1 M NaPB solution.

CoHCF has a face-centred cubic lattice crystal structure with a cell constant a of about 10.2 \AA ; Co(II) and Fe(II) or Fe(III), bridged by a CN^- group [36], appear alternatively

at the sites of small cubes. Owing to the rigidity of the crystal lattice of the CoHCF film, the diffusion of cobalt ions in it is very difficult. Only counter-ions, such as K^+ , Na^+ etc., are transported through the CoHCF film during the electrochemical redox process in order to maintain electroneutrality. The new cathodic peak at a potential of about $+0.59 \text{ V}$ which appears on the cyclic voltammograms of Fig. 1(B) is the result of cation transfer in the CoHCF film as proposed by Dong and Jin [37] for MoHCF film. Hence the hydrated ionic radii of counter-ions inevitably affects the behaviour of the CoHCF film. Therefore the difference between the formal potentials of CoHCF in KPB and NaPB solutions can be explained in terms of the different transfer rate of counter-ions in CoHCF. The transport of K^+ in CoHCF film is more difficult than that of Na^+ because the hydrated ionic radius of K^+ (1.33 \AA) is larger than that of Na^+ (0.95 \AA).

3.3. Effect of electrolyte concentration on the CoHCF|Au electrode

Cyclic voltammograms of a CoHCF|Au microelectrode in three different concentrations of NaCl (pH 7.0) are shown in Fig. 2. With decreasing concentration of electrolyte, the redox peaks shift in the negative direction and the peak currents decrease simultaneously. The formal potential is $+0.39 \text{ V}$ in 1 M NaCl solution, whereas in 0.01 M NaCl solution it shifts to $+0.29 \text{ V}$. The following equation can be obtained by treating the film as a solid solution as in the case of PB film [38]:

$$E = E_M^{0'} + \frac{RT}{nF} \ln \frac{a_{\text{CoHCF}_{\text{ox}}} a_{\text{M}^+}}{a_{\text{CoHCF}_{\text{red}}}} \quad (2)$$

$\text{M} = \text{Na}, \text{K}, \dots$

Thus the shift of potential is due to the change in the activity of Na^+ in solution. The reversibility of CoHCF|Au

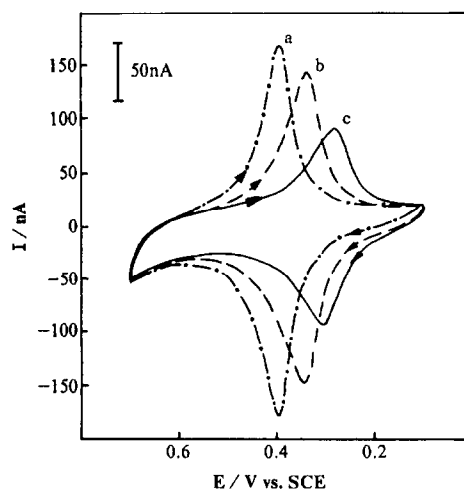


Fig. 2. Cyclic voltammograms of the modified microelectrode in (a) 1.0 M, (b) 0.1 M and (c) 0.01 M NaCl solution (pH 7.0).

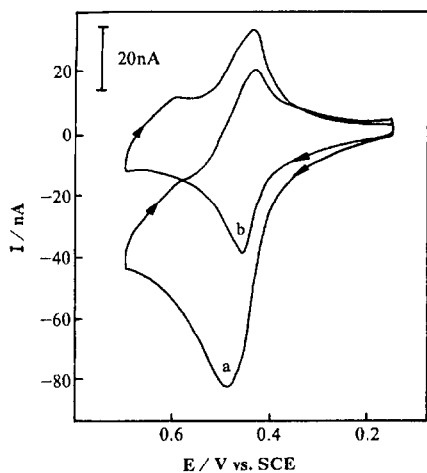


Fig. 3. Catalytic oxidation of NADH at a modified microelectrode in 0.1 M KPB (pH 7.0) (a) with 2.0 mM NADH and (b) without NADH at a scan rate of 50 mV s^{-1} .

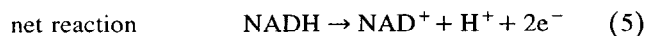
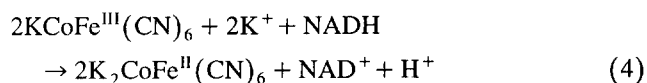
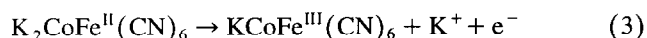
is also affected by the electrolyte concentration. In 1 M NaCl the electrode process is almost reversible and the peak separation is 2 mV at a scan rate of 50 mV s^{-1} , whereas in 0.01 M NaCl the separation is 28 mV and the reversibility is decreased.

3.4. The stability of the modified electrode

The stability of the modified electrode was studied by exposing it in air or storing it in buffer solution for a period of time, and then recording the cyclic voltammograms. The experimental results indicate that the CoHCF|Au is not affected by air. Furthermore, there is no loss of redox activity after storage in the buffer solution for about a week. In addition, there were no changes in the height and separation of the cyclic voltammogram after 100 cycles repetitive scanning in buffer solution.

3.5. Catalytic oxidation of NADH at the modified electrode

Fig. 3(a) shows the cyclic voltammogram of the CoHCF|Au microelectrode in 0.1 M KPB solution containing 2.0 mM NADH. It can be seen that there is a large increase in the anodic peak current, corresponding to the oxidation of hexacyanoferrate(II) to hexacyanoferrate(III), compared with the voltammogram in buffer solution without NADH (Fig. 3(b)). The reason is that the NADH in the solution reduces the hexacyanoferrate(III) to hexacyanoferrate(II). This process increases the anodic peak current, while the cathodic peak current is smaller than that in the absence of NADH. The overall process according to an EC catalytic mechanism can be expressed as



The anodic peak potential for the oxidation of NADH at the CoHCF|Au electrode is about +0.48 V in 0.1 M KPB solution. At the bare gold electrode, the anodic peak potential is at ca. +0.85 V [39]. Thus a decrease in the overpotential of approximately 370 mV is achieved. The scan rate dependence of cyclic voltammograms for the CoHCF|Au microelectrode in 0.1 M KPB solution containing 2.0 mM NADH is shown in Fig. 4. As the scan rate increases, the anodic peak potential shifts slightly in the positive direction; for example, the anodic potential is +0.51 V at 20 mV s^{-1} , and shifts to +0.53 V at 100 mV s^{-1} . The anodic currents increase linearly with the square root of scan rate. Further experimental results show that the steady-state currents measured using chronoamperometry at +0.50 V are proportional to the concentration of NADH in the range 0.5–6.0 mM with a correlation coefficient of 0.98. The linear relationship between the steady-state currents and the concentration of NADH establishes the basis for the determination of NADH in a given sample. The use of the new modified electrode to determine NADH in a real sample is currently being studied.

Fig. 5 shows the cyclic voltammograms of the CoHCF|Au electrode in 0.1 M NaPB solution with 2.0 mM NADH (Fig. 5(a)) and without NADH (Fig. 5(b)). The anodic peak current shows a large increase in NADH solution for the same reason as in the KPB solution. The anodic peak potential of NADH at CoHCF|Au is located at about +0.54 V, the decrease of overpotential is 310 mV, and the anodic peaks of NADH and the hexacyanoferrate(II) are separated by about 200 mV. However, in KPB solution, the two anodic peaks overlap and the total anodic peak shifts in the positive direction by about 26 mV in the presence of NADH (see Fig. 3). This difference between the two electrolytes is probably due to the change in the transport rate of K^+ and Na^+ in CoHCF film. In addition, the electrostatic factor, the ionic polarizabilities and the

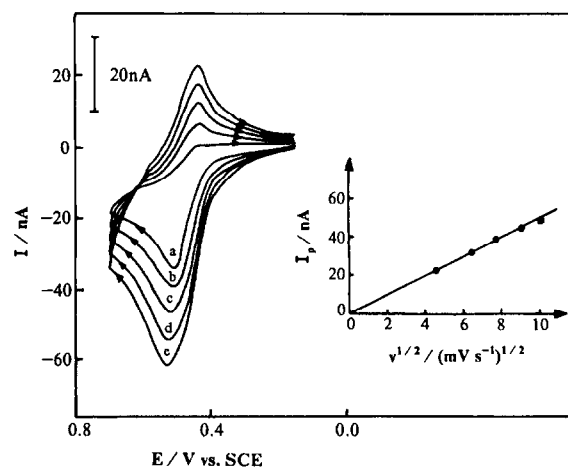


Fig. 4. Cyclic voltammograms of the modified microelectrode in 0.1 M KPB solution (pH 7.0) containing 2.0 mM NADH at scan rates ν of (a) 20, (b) 40, (c) 60, (d) 80 and (e) 100 mV s^{-1} . The inset shows the plot of I_{pa} vs. $\nu^{1/2}$.

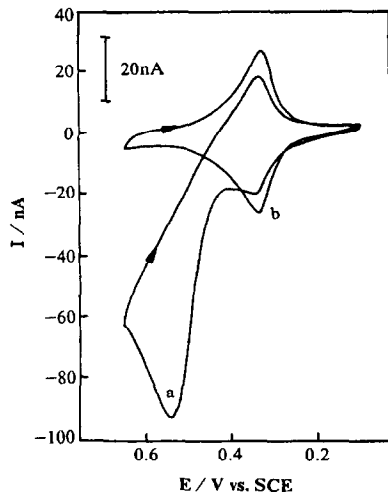


Fig. 5. Catalytic oxidation of NADH at the modified microelectrode in 0.1 M NaPB (pH 7.0) (a) with 2.0 mM NADH and (b) without NADH at a scan rate of 50 mV s^{-1} .

structural disorder of the microcrystalline deposit can also affect ion migration through the CoHCF film and consequently the electrocatalytic characteristic of the oxidation of NADH.

The cyclic voltammograms of the electrode in 0.1 M NaPB solution containing 2.0 mM NADH at various scan rates are shown in Fig. 6. The results are similar to those obtained in 0.1 M KPB solution. The fact that the peak currents depend on the scan rate and the anodic peak potential shifts with increasing scan rate indicates that the overall electrocatalytic process may be controlled by the diffusion of NADH in solution and the cross-exchange reaction between NADH and the redox site of the CoHCF film. Thus, the mechanism seems to be complicated.

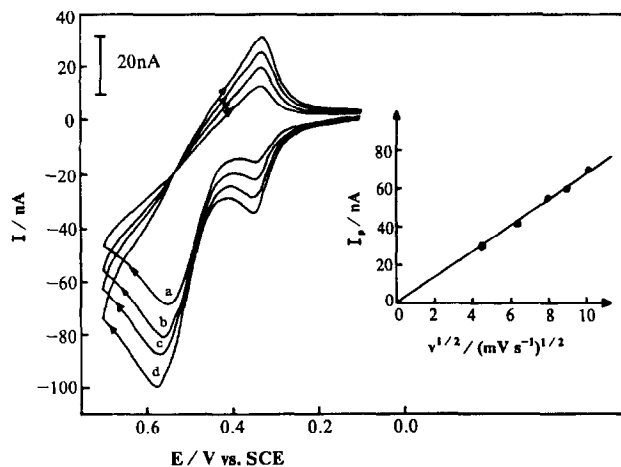


Fig. 6. Cyclic voltammograms of the modified microelectrode in 0.1 M NaPB solution (pH 7.0) containing 2.0 mM NADH at scan rates v of (a) 20, (b) 40, (c) 60, (d) 80 and (e) 100 mV s^{-1} . The inset shows the plot of I_{pa} vs. $v^{1/2}$.

3.6. Kinetics of the electrocatalytic oxidation of NADH

It is difficult to analyse the electrocatalytic process quantitatively by cyclic voltammetry alone in the present case, because the rate-controlled process is complicated. However, with rotating-disc electrode measurements the electrode is kept at a stationary potential and a steady state is attained. Thus the rates of mass transfer at the surface of the rotating-disc electrode are much larger than those of diffusion. Therefore the relative contribution of the effect of mass transfer to electron transfer kinetics is smaller.

In the present case, the catalytic process was studied in KPB solution with a rotating-disc electrode as an example to obtain the kinetic parameters. The rotating-disc electrode was kept at $+0.50 \text{ V}$ in the potential range of the plateau obtained in the voltammetric curve at a lower scan rate. The anodic currents of NADH increase with increasing rotational speed, but obvious deviations from the theoretical line are observed at high rotational speed, which indicates that the limiting currents are controlled by a kinetic step. The limiting current I_L corresponding to the mediated reaction is a function of the Levich current I_{Lev} representing the mass transfer of NADH in the solution and the kinetic current I_K corresponding to the electron cross-exchange between NADH and the CoHCF redox site. The catalytic reaction rate between the oxidized CoHCF and NADH can be obtained from the Koutecky–Levich plot using the following expression:

$$1/I_L = 1/I_{Lev} + 1/I_K \quad (6)$$

and

$$I_{Lev} = 0.62 nFA D^{2/3} \nu^{-1/6} c_{NADH} \omega^{1/2} \quad (7)$$

$$I_K = nFAk\Gamma c_{NADH} \quad (8)$$

where c_{NADH} is the bulk concentration of NADH, ω is the rotational speed, ν is the hydrodynamic viscosity, Γ is the

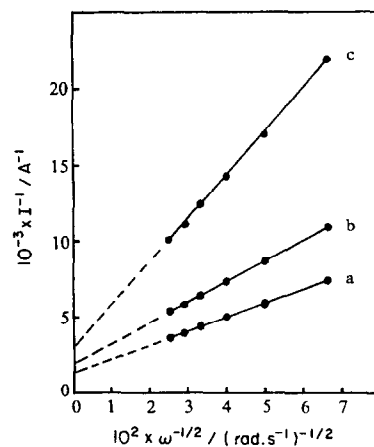


Fig. 7. Koutecky–Levich plots for the oxidation of NADH in 0.1 M KPB solution (pH 7.0) containing (a) 1.5, (b) 1.0 and (c) 0.5 mM NADH at a modified microelectrode with $\Gamma = 5.0 \times 10^{-8} \text{ mol cm}^{-2}$.

surface coverage of CoHCF, k is the rate constant of Eq. (4) and all other parameters have their usual meanings.

Koutecky–Levich plots are shown in Fig. 7. Both the slopes and the intercepts of the lines are in inverse proportion to the concentration of NADH in accord with Eqs. (6)–(8). The rate constant k can be calculated from the intercept of the Koutecky–Levich plot and is found to be $3.8 \times 10^3 \text{ M}^{-1} \text{ s}^{-1}$, $3.5 \times 10^3 \text{ M}^{-1} \text{ s}^{-1}$ and $3.1 \times 10^3 \text{ M}^{-1} \text{ s}^{-1}$ for NADH concentrations of 0.5 mM, 1.0 mM and 1.5 mM respectively. These values are comparable with those previously reported for the electrocatalytic oxidation of NADH at the electrode modified with the other mediators such as 1,2-benzophenoxazine-7-one ($8 \times 10^2 \text{ M}^{-1} \text{ s}^{-1}$) [18,20], 5-methylphenazinium- or tetrathiafulvalene-tetracyanoquinodimethane radical salts ($1.5 \times 10^3 \text{ M}^{-1} \text{ s}^{-1}$) [21], 4-methyl catechol ($3.3 \times 10^3 \text{ M}^{-1} \text{ s}^{-1}$) [23] and poly(thionine) ($2.1 \times 10^3 \text{ M}^{-1} \text{ s}^{-1}$) [30].

References

- [1] P.K. Ghosh and A.J. Bard, *J. Am. Chem. Soc.*, 105 (1983) 5692.
- [2] C.G. Murray, R.J. Nowak and D.R. Rolish, *J. Electroanal. Chem.*, 164 (1984) 205.
- [3] P.J. Kulesza and L.R. Faulkner, *J. Am. Chem. Soc.*, 110 (1988) 4905.
- [4] F. Opekar, *J. Electroanal. Chem.*, 260 (1989) 451.
- [5] B. Keita and L. Nadjio, *J. Electroanal. Chem.*, 269 (1989) 447.
- [6] M. Jiang and Z. Zhao, *J. Electroanal. Chem.*, 292 (1990) 281.
- [7] M. Jiang, X. Zhou and Z. Zhao, *J. Electroanal. Chem.*, 292 (1990) 289.
- [8] F. Li and S. Dong, *Electrochim. Acta*, 32 (1987) 1511.
- [9] K. Itaya, K. Shibayama, H. Akahoshi and S. Toshima, *J. Appl. Phys.*, 52 (1982) 804.
- [10] Z. Gao, X. Zhou, G. Wang, P. Li and Z. Zhao, *Anal. Chim. Acta*, 244 (1991) 39.
- [11] V.D. Neff, *J. Electrochem. Soc.*, 132 (1985) 1382.
- [12] J.S. Bergel and M. Comtat, *Anal. Biochem.*, 179 (1989) 382.
- [13] J.M. Laval, C. Bourdillon and J. Moiroux, *J. Am. Chem. Soc.*, 106 (1984) 4701.
- [14] P.J. Elving, W.T. Bresnahan, J. Moiroux and Z. Samec, *Bioelectrochem. Bioenerg.*, 9 (1982) 365.
- [15] H. Jaegfeldt, T. Kuwana and G. Johansson, *J. Am. Chem. Soc.*, 105 (1983) 1805.
- [16] H. Jaegfeldt, A. Torstensson, L. Gorton and G. Johansson, *Anal. Chem.*, 53 (1981) 1979.
- [17] L. Gorton, G. Johansson and A. Torstensson, *J. Electroanal. Chem.*, 196 (1985) 81.
- [18] L. Gorton, A. Torstensson, H. Jaegfeldt and G. Johansson, *J. Electroanal. Chem.*, 161 (1984) 103.
- [19] L. Gorton, *J. Chem. Soc. Faraday Trans. 1*, 82 (1986) 1245.
- [20] B. Persson and L. Gorton, *J. Electroanal. Chem.*, 292 (1990) 115.
- [21] W.J. Albery and P.N. Bartlett, *J. Chem. Soc. Chem. Commun.*, (1984) 234.
- [22] C. Ueda, D.C.-S. Tse and T. Kuwana, *Anal. Chem.*, 54 (1982) 850.
- [23] M. Fukui, C. Kitani, C. Degrand and L.L. Miller, *J. Am. Chem. Soc.*, 104 (1982) 28.
- [24] K. Ravichandran and R.P. Baldwin, *J. Electroanal. Chem.*, 126 (1981) 293.
- [25] H. Huck and H.L. Schmidt, *Angew. Chem.*, 93 (1981) 421.
- [26] A. Torstensson and L. Gorton, *J. Electroanal. Chem.*, 130 (1981) 199.
- [27] K. Hajizadeh, H.T. Tang, H.B. Halsall and W.R. Heineman, *Anal. Lett.*, 24 (1991) 1453.
- [28] N.F. Atta, A. Galal, A.E. Karagozler, H. Zimmer, J.F. Rubinson and H.B. Mark Jr., *J. Chem. Soc. Chem. Commun.*, (1990) 1347.
- [29] G. Arai, M. Matsushita and I. Yasumori, *Nippon Kagaku Kaishi*, 5 (1985) 894.
- [30] T. Ohsaka, K. Tanaka and K. Tokuda, *J. Chem. Soc. Chem. Commun.*, (1993) 222.
- [31] F. Xu, H. Li, S.J. Cross and T.F. Guarr, *J. Electroanal. Chem.*, 368 (1994) 221.
- [32] C.X. Cai, H.X. Ju and H.Y. Chen, *Acta Chim. Sin.*, 53 (1995) 281.
- [33] Z. Gao, G. Wang, P. Li and Z. Zhao, *Electrochim. Acta*, 36 (1990) 147.
- [34] E. Laviron, *J. Electroanal. Chem.*, 101 (1979) 19.
- [35] A.J. Bard and L.R. Faulkner, *Electrochemical Methods, Fundamentals and Applications*, Wiley, New York, 1980, Ch. 12.
- [36] A.G. Sharpe, *The Chemistry of Cyano Complexes of the Transition Metals*, Academic Press, New York, 1976, Ch. 7.
- [37] S. Dong and Z. Jin, *J. Electroanal. Chem.*, 256 (1988) 193.
- [38] D. Eillis and V.D. Neff, *J. Phys. Chem.*, 85 (1981) 1225.
- [39] C.X. Cai, H.Y. Chen and H.X. Ju, *Anal. Chim. Acta*, in press.